한국소음진동공학회 창립10주년 기념 소음진동학술대회논문집, pp. 1051~1057.

보조동력 개스터빈 로터-베어링 시스템에서 체결축의 로터다이나믹 영향

Rotordynamic Influences of a Tie Shaft in a APU Gas Turbine Rotor-Bearing System

이 안 성* · 이 영 섭**
An Sung Lee and Young-Seob Lee

ABSTRACT

A projected 100 kW APU gas turbine rotor-bearing system has a main outer shaft, which is composed of some numbers of segmented sections for manufacturing and assembly conveniences. For a secure assembly of the segmented sections a tie shaft or inner shaft is installed inside of the outer shaft and a tensional axial preload of 50,000 N is provided to it. In this paper it is intended to set-up a sound modeling method of the APU rotor system, and particularly, the influences of the tie shaft on the rotordynamic characteristics of the entire APU gas turbine rotor-bearing system are investigated. Analysis results show that as a conservative design practice the inner tie shaft should be actively modeled in the rotordynamic analysis of the APU rotor-bearing system, and its effects on the dynamic behaviors of the outer shaft should be thoroughly design-reviewed.

1. Introduction

In aerospace or compact high performance gas turbines it is not unusual to find that their main rotors are made up of many segmented sections and that the rotors are tied as one pieces by tie bolts or inner shafts with high tensional axial preloads. These tie shafts and many discontinuous connections in general add some uncertainties or errors to analytical models of the rotors.

In analyzing rotor-bearing systems the transfer matrix method [1-3] and the finite element method [4-6] have been being widely used. Generally speaking, the former is more advantageous in element formulations and computation times than the latter but more disadvantageous in modeling complex configurations and solution procedures. With fast technology advances in computer hardwares the finite element method is gaining more popularities as a rotordynamic analysis tool these days.

In this study a projected 60,000 rpm 100 kW APU gas turbine rotor-bearing system

* Korea Institute of Machinery and Materials
** Samsung Aerospace

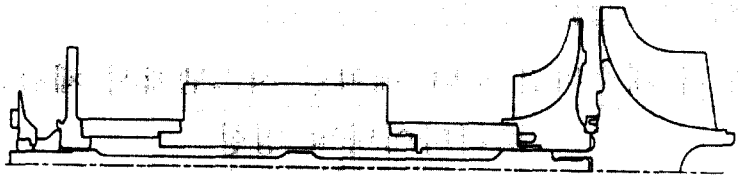

Fig. 1 Schematic of the 100 kW prototype APU rotor.

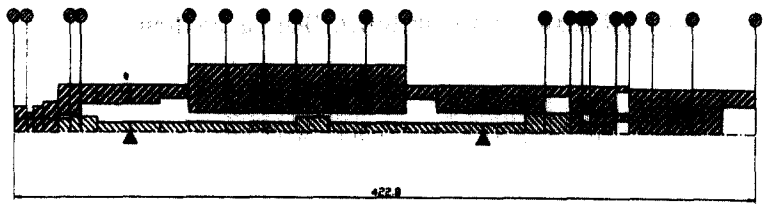

Fig. 2 An equivalent finite element model of the prototype APU rotor.

shown in Fig. 1 has a main outer shaft, which is composed of some numbers of segmented sections for manufacturing and assembly conveniences. For a secure assembly of the segmented sections a tie shaft or inner shaft is installed inside of the outer shaft and a tensional axial preload of 50,000 N is provided to it. It is intended to set-up a sound modeling method of the APU rotor system having the inner tie shaft and many discontinuous connections. And the rotordynamic characteristics of the prototype APU rotor-bearing system, whose bearings are of air-foil type, is investigated to particularly evaluate the influences of the inner tie shaft on the rotordynamic behaviors of the outer main rotor shaft. The rotor-bearing system is modeled with the finite element method.

2. Modeling and solution procedure

In modeling two modeling methods are considered. One is a conventional single shaft modeling, where stiffness and inertia matrices of the inner shaft are added to corresponding those of the outer shaft. The other is a dual shaft modeling, where the inner shaft is provided at its each node with independent degrees of freedom apart from those of the outer shaft.

The tensional axial force of the inner shaft and the compressional axial force of the outer shaft can be considered in the modeling using the following strain energy:

$$U_S = -\frac{1}{2} F_A \int_0^l \left[\left(\frac{\partial u}{\partial Z} \right)^2 + \left(\frac{\partial v}{\partial Z} \right)^2 \right] dZ \quad (1)$$

where F_A is a compressional axial force, and u and v are translational X and Y displacements at a location Z along the shaft element.

The assembled resultant equation of motion of the entire rotor-bearing system is expressed as

$$[M]\{\ddot{q}\}+[C]\{\dot{q}\}+[K]\{q\} = \{Q\} \quad (2)$$

where $[M]$, $[C]$, and $[K]$ are the mass, damping, and stiffness matrices, and $\{q\}$ and $\{Q\}$ are the column vectors of generalized displacements and forces, respectively. The gyroscopic components are included in $[C]$.

For a free vibration analysis Eqn. (2) may be expressed in the state-space form as

$$\begin{Bmatrix} \{\dot{q}_2\} \\ \{\dot{q}_1\} \end{Bmatrix} = [A] \begin{Bmatrix} \{q_2\} \\ \{q_1\} \end{Bmatrix} \quad (3)$$

where $[A]$ is the dynamic matrix of the system, and $\{q_1\} = \{q\}$ and $\{q_2\} = \{\dot{q}\}$. $[A]$ is defined as

$$[A] = \begin{bmatrix} -[M]^{-1}[C] & -[M]^{-1}[K] \\ [I] & [0] \end{bmatrix} \quad (4)$$

The eigenvalues and eigenvectors are calculated from the dynamic matrix to give whirl natural frequencies and mode shapes.

Unbalance response of the system is derived by substituting the following generalized unbalance force and assumed solution into Eqn. (2):

$$\{Q\} = \Omega^2\{U_C\}\cos\Omega t + \Omega^2\{U_S\}\sin\Omega t \quad (5)$$

$$\{q\} = \{a\}\cos\Omega t + \{b\}\sin\Omega t \quad (6)$$

where $\{U_C\}$ and $\{U_S\}$ are the coefficient vectors of unbalance forcing, and $\{a\}$ and $\{b\}$ are the coefficient vectors of unbalance solution. After some algebra the following unbalance matrix equation is obtained:

$$\begin{bmatrix} [K]-\Omega^2[M] & \Omega[C] \\ -\Omega[C] & [K]-\Omega^2[M] \end{bmatrix} \begin{Bmatrix} \{a\} \\ \{b\} \end{Bmatrix} = \Omega^2 \begin{Bmatrix} \{U_C\} \\ \{U_S\} \end{Bmatrix} \quad (7)$$

Then, $\{a\}$ and $\{b\}$ of the unbalance response is calculated from Eqn. (7).

3. Results and discussions

Figs. 1 and 2 show a schematic of the prototype APU rotor and its equivalent finite element model. Two air foil bearing locations are marked in Fig. 2 as hatched triangle supports. Applying the foregoing single and dual shaft modelings detailed whirl mode and unbalance response analyses have been carried out with the prototype APU rotor-bearing system. In the analyses the following air-foil bearing dynamic coefficients have been used: $K_B = 2\times10^6\ N/m$ and $C_B = 1\times10^3\ N\cdot s/m$ for the LHS bearing, and $K_B = 8\times10^6\ N/m$ and $C_B = 2\times10^3\ N\cdot s/m$ for the RHS bearing.

3.1 Whirl mode shapes and critical speeds

For the single shaft modeling, whirl mode analysis results are shown in Figs. 3-5, where the effect of the inner shaft tension of 50,000 N has not been considered in this analysis. The 1st mode in Fig. 3 and 2nd mode in Fig. 4 are rigid

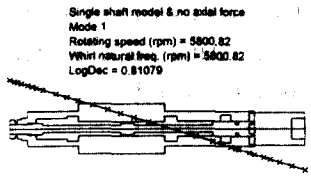

Fig. 3 1st critical mode of the APU rotor with the single shaft model.

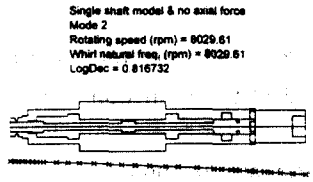

Fig. 4 2nd critical mode of the APU rotor with the single shaft model.

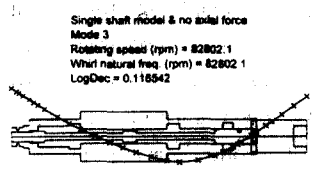

Fig. 5 3rd critical mode of the APU rotor with the single shaft model.

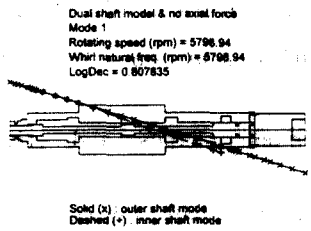

Fig. 6 1st critical mode of the APU rotor with the dual shaft model.

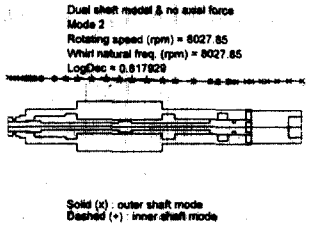

Fig. 7 2nd critical mode of the APU rotor with the dual shaft model.

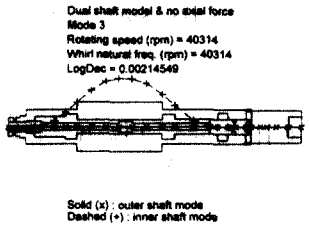

Fig. 8 3rd critical mode of the APU rotor with the dual shaft model

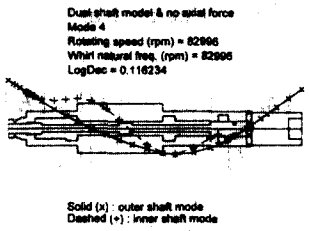

Fig. 9 4th critical mode of the APU rotor with the dual shaft model.

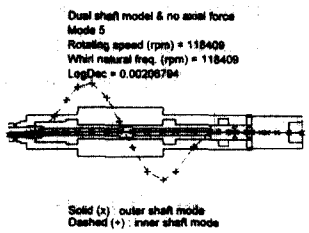

Fig. 10 5th critical mode of the APU rotor with the dual shaft model.

body modes, and have the critical speeds of 5,801 and 8,030 rpm. The 3rd mode in Fig. 5 is a bending mode, and has the critical speed of 82,802 rpm. As the APU has the rated speed of 60,000 rpm, the 3rd critical speed has the sufficient separation margin.

For the dual shaft modeling with no inner shaft tension considered, whirl mode analysis results are shown in Figs. 6-10. The 1st mode in Fig. 6 and 2nd mode in Fig. 7, which are rigid body modes, have the critical speeds of 5,799 and 8,028 rpm. They are practically the same as those for the single shaft modeling. For the 3rd mode in Fig. 8 and 5th mode in Fig. 10 the inner shaft is greatly excited whereas the outer shaft is little excited. Therefore, they are determined as the inner shaft bending modes. Their critical speeds are 40,314 and 118,409 rpm. Here, since the 3rd critical speed is within the operating speed range and its LogDec (Logarithmic Decrement) is very low, its effect needs to be further investigated by unbalance analysis. On the other hand, for the 4th mode in Fig. 9 the outer shaft is greatly excited and the outer shaft mode shape is almost the same as the 3rd mode shape for the single shaft modeling. Therefore, the 4th mode for the present case is determined as the outer shaft bending mode. Its critical speed is 82,996 rpm, which is very close to that for the single shaft modeling.

In Table 1 are summarized the critical speeds obtained for the various modeling cases. For the dual shaft modeling with the inner shaft tension considerd, the 3rd and 5th critical speeds due to the inner shaft bending modes increase greatly and particularly the 3rd critical speed is predicted as 56,184 rpm, which are very close to the rated speed.

3.2 Unbalance Responses

Unbalance response analyses have been performed with two times of the API allowable residual unbalance limit, which has been attached to the generator and turbine in-phase.

For the single shaft modeling, overall unbalance responses are all predicted to be quite satisfactory, having less than 4 μm Pk-to-Pk vibrations at the rated speed of 60,000 rpm and at the two passing critical speeds of rigid body modes.

For the dual shaft modeling with no inner shaft tension considered, unbalance response analysis results are shown in Figs. 11-15. Unbalance response characteristic over 0 to 70,000 rpm is given in Fig. 11. Three response peaks are observed due to the two rigid body modes and one inner shaft bending mode criticals. Figs. 12 and 13 show unbalance responses at the 1st and 2nd criticals, and responses throughout the entire rotor locations are all less than 4 μm Pk-to-Pk. Fig. 14 shows unbalance response at the 3rd critical speed of the inner shaft bending mode. Due to the inner shaft resonance the inner shaft response, which is marked as a dashed line, can reach as high as 600 μm Pk-to-Pk. The outer shaft response can grow up to 13 μm Pk-to-Pk due to the influence of the inner shaft resonance. Fig. 15 shows unbalance response at the rated speed, and vibration level is predicted as less than 2 μm Pk-to-Pk.

For the dual shaft modeling with the inner shaft tension considered, unbalance

Table 1 Critical speeds of the APU rotor-bearing system, depending on the different modelings.

Analytical Results Critical speed (rpm)			Dominant mode
Single shaft model	Dual shaft model		
	With no axial force	With axial force	
5,801	5,799	6,015	Rigid body
8,030	8,028	8,027	Rigid body
	40,314	56,184	Inner shaft bending
82,802	82,996	83,019	Outer shaft bending
	118,409	142,665	Inner shaft bending
173,815	174,420	174,470	Outer shaft bending

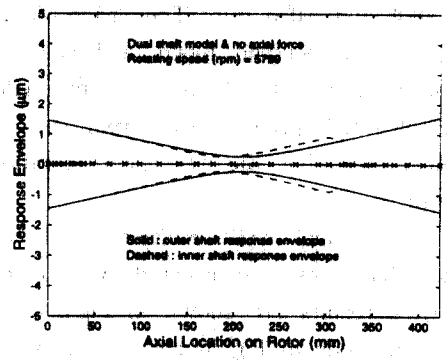

Fig. 12 Unbalance response at the 1st rigid-mode critical speed of the APU rotor with the dual shaft model.

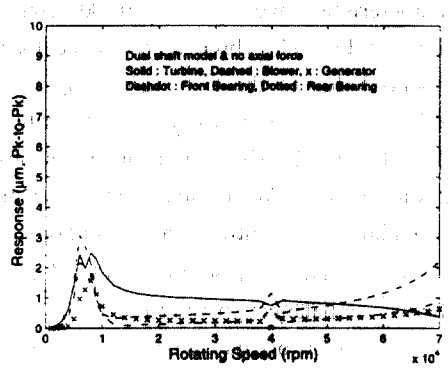

Fig. 11 Unbalance response over the full speed range of the APU rotor with the dual shaft model.

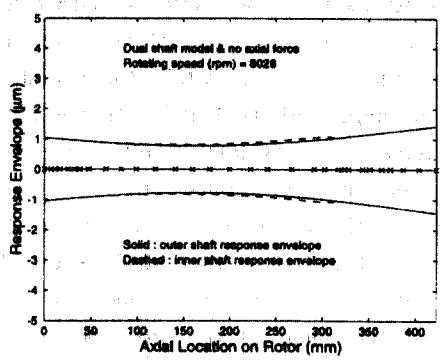

Fig. 13 Unbalance response at the 2nd rigid-mode critical speed of the APU rotor with the dual shaft model.

responses at the 1st and 2nd criticals are all less than 4 μm Pk-to-Pk, again. However, at the 3rd critical speed of the inner shaft bending mode the inner shaft response can increase as high as 200 μm Pk-to-Pk, and the outer shaft response can grow up to a little over 4 μm Pk-to-Pk again due to the influence of the inner shaft resonance.

4. Conclusions

It has been pursued to set-up an accurate modeling method of the prototype APU rotor system, having the inner tie shaft and many discontinuous connections, and particularly, the influences of the tie

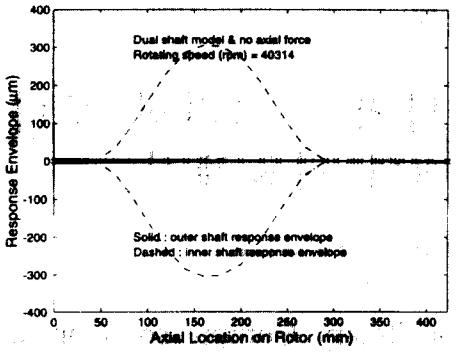

Fig. 14 Unbalance response at the 3rd inner shaft critical speed of the APU rotor with the dual shaft model.

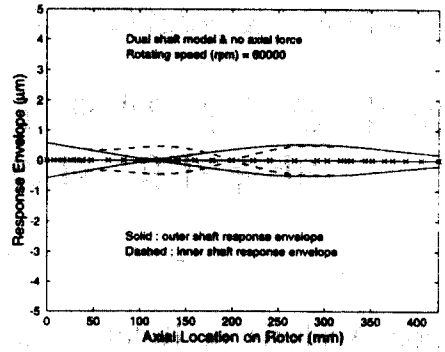

Fig. 15 Unbalance response at the rated speed of 60,000 rpm of the APU rotor with the dual shaft model.

shaft on the rotordynamic characteristics of the entire APU rotor-bearing system have been investigated. The dual shaft modeling based on the finite element method, where the inner shaft is provided at its each node with independent degrees of freedom apart from those of the outer shaft, has been proposed in the analyses.

The dual shaft modeling has shown that the APU system has one inner shaft bending mode 3rd critical speed before it reaches its rated speed of 60,000 rpm, which has not been predicted by the conventional single shaft modeling practice. Unbalance analysis results have shown that the main outer shaft may have some amplified responses due to the inner shaft resonnance at the 3rd critical speed. This characteristic needs to be further analytically investigated and experimentally confirmed in the future work to ensure smooth operation free of high vibrations.

References

[1] Rao, J. S., 1983, *Rotor Dynamics*, A Halsted Press Book.

[2] Pestel, E. C. and Leckie, F. A., 1963, Matrix Methods in Elasto Mechanics, McGraw-Hill Book Co., Inc.

[3] Lund, J. W. and Orcutt. F. K., 1967, "Calculations and Experiments on the Unbalance Response of a Flexible Rotor," ASME Trans., Journal of Engineering for Industry., pp. 785-796.

[4] Zorzi, E. S. and Nelson, H. D., 1977, "Finite Element Simulation of Rotor-Bearing Systems with Internal Damping," ASME Trans., *Journal of Engineering for Power*, Vol. 99, pp. 71-76.

[5] Lalanne, M. and Ferraris, G., 1990, *Rotordynamics Prediction in Engineering*, John Wiley and Sons.

[6] Özgüven, H. N. and Özkan Z. L., 1984, "Whirl Speeds and Unbalance Response of Multibearing Rotors Using Finite Elements," ASME Trans., *Journal of Vibration, Acoustics, Stress, and Reliability in Design*, Vol. 106, pp. 72-79.